

Article

The Decoloration of Anionic and Cationic Dyes Using ZnO and ZnO-Cu₂O

Jiang Dong Dai, Luo Gan, Hai Yan Zhang and Chun Ming Liu *

School of physics, University of electronic science and technology of China, Chengdu 610054, China; dajiade2000@163.com (J.D.D.); 201821120114@std.uestc.edu.cn (L.G.); 15520793203@163.com (H.Y.Z.)

* Correspondence: cmliu@uestc.edu.cn; Tel.: +86-028-8320-2590

Received: 29 March 2019; Accepted: 26 April 2019; Published: 28 April 2019



Abstract: ZnO and ZnO-Cu₂O were grown on aluminum foam using hydrothermal method. Due to the positively charged sites on the surface, both ZnO and ZnO-Cu₂O show higher adsorption capability towards anionic dyes, but poorer adsorption capability towards cationic dyes. The adsorption ability of ZnO-Cu₂O is smaller than that of ZnO since there is a depletion layer at the interface. In order to decolorize cationic dyes, ZnO and ZnO-Cu₂O are used as sono-catalyst with ultrasonic irradiation. The ZnO-Cu₂O is better than ZnO in sono-catalysis decoloration of cationic dyes. This may be due to the enhanced piezoelectricity and electrochemical activity, as the free electrons in ZnO are reduced in the depletion layer.

Keywords: decoloration; dyes; ZnO; ZnO-Cu₂O; adsorption; sono-catalyst

1. Introduction

Dye-related environmental pollution is a serious problem. Dyes are becoming severe contaminants due to their toxicity and low biodegradability. Dyes are widely used in textile, paper, leather, food, plastics, cosmetics, and pharmaceutical industries. In order to eliminate dye pollution, ZnO is widely investigated as photo-catalysis [1,2], adsorbents [2–4], vibration catalysis [5], thermo-catalysis [6], piezo-photo-catalysis [7], photo-electro-catalytic [8], sono-catalysis [9], and photo-sono-catalysis [9]. Among all these methods, adsorption is considered as one of the most attractive methods due to its simplicity, low cost, ease of operation, and efficiency [10]. However, due to the positively charged sites at a ZnO surface, ZnO only exhibits high adsorption capability towards some negatively charged dyes (anionic dyes), but has poor adsorption capability towards positive charged dyes (cationic dyes) [3]. It is evident that a new method other than adsorption should be taken to eliminate positive charged dyes.

Cu₂O is one of the few materials showing a mechano-catalytic effect [11]. Cu₂O was used to split water [11] and mineralize dyes [12]. Furthermore, ZnO-Cu₂O heterojunction shows enhanced photo-catalytic performance and stable and fast response photodetectors [13–15]. The p-n junction structure of Cu₂O-ZnO provides a depletion layer at the interface of junction [14]. The depletion layer was demonstrated to be beneficial for the enhancement of the output of piezoelectricity [16]. The piezoelectricity is useful in vibration catalysis [5] and piezo-photo-catalysis [7]. The positive–negative charges are easier to get apart because of the small exciton binding energy with built-in polarization due to piezoelectric effect. The negative (or positive) charges on the surface can produce superoxide radicals (or hydroxyl radicals) to degrade dyes [5]. The piezoelectric field can separate the photo-generated electrons/holes by driving them to migrate along opposite directions [7].

While ZnO-Cu₂O heterojunction has been widely studied, there is little work on vibration catalysis or sono-catalysis. To our knowledge, most work about the mechano-catalytic effect and piezo-catalysis is focused on single-phase material [5,11]. There is little work about the influence of depletion layers at the interface on sono-catalysis and piezo-catalysis. It is interesting to study whether the

enhancement of piezoelectricity of ZnO-Cu₂O heterojunction is beneficial for the decoloration of dyes. The adsorption of dyes using ZnO and ZnO-Cu₂O as adsorbents is firstly investigated in this paper. Then the decolorization of cationic dyes using ZnO and ZnO-Cu₂O as a sono-catalyst under ultrasonic irradiation is studied. Ultrasonic irradiation is widely used as mechanical energy in the study of sono-catalysis and piezo-catalysis [5,7]. Ultrasonic irradiation has many advantages including high penetrability in a water medium and no generation of secondary pollutants [17].

2. Experiments

The aluminum (Al) foam is available from SuZhou JiaYiSheng electronics CO., LTD (SuZhou, JiangSu, China). The porosity of the sample is about 68–78%. The surface area of foam is about 0.3 m²/g. The size of the alumina foam sample is about 3 × 40 × 40 mm³. The foam sample is in turn cleaned in ethanol and deionized water using an ultrasonic cleaner. ZnO nano-sheets were fabricated on Al foam substrate by hydrothermal method. The precursor solution for growth ZnO nano-sheets was prepared by equal volume mixing of zinc nitrate water solution (50 mL, 50 mmol L⁻¹) and hexamethylenetetramine water solution (50 mL, 15 mmol L⁻¹). The substrate was put into the precursor solution and kept at 80 °C for 6 h to grow ZnO nano-sheets. After the growth of ZnO nano-sheets, the substrate was taken out and rinsed using deionized water and dried in air.

The precursor solution for growth Cu₂O was prepared by the mixing of cupric acetate water solution (50 mL, 50 mmol L⁻¹) and hexamethylenetetramine water solution (50 mL, 15 mmol L⁻¹). The Al foam substrates with and without ZnO nano-sheets were put into the precursor solution and kept at 60 °C for 2–6 h to grow Cu₂O and ZnO-Cu₂O samples. The samples' stoichiometry was measured by X-ray photoelectron spectroscopy (XPS; Kratos X SAM 800, Kratos Analytical Ltd, Manchester, UK).

Methyl orange (MO) and methylene blue (MB) aqueous solution were used as anionic dye and cationic dye for decolorization, respectively.

The optical absorption of MO and MB aqueous solution was measured by Ultraviolet-Vis spectrophotometer (SHIMADZU UV-2550, Shimadzu Corporation, Kyoto, Japan). The optical absorption of MO solution and MB solution with various concentrations was measured. It is found that the intensity of the optical absorption peak, at about 463 (662) nm, is proportional to the MO (MB) concentration. Thus the intensity of the optical absorption peak at 463 nm (662 nm) is used to calculate the concentration of the MO (MB) solution. In the decoloration experiments, the initial concentration of the MO and MB water solution is about 20 mg/l. The ultrasonic irradiation is performed in a KQ-300VDE ultrasonic cleaner. The power and frequency of the ultrasonic cleaner is about 100 W and 100 kHz, respectively. The samples' morphology is measured using Inspect F50 scanning electron microscopy (SEM). The atomic ratio of sample is measured using energy disperse spectroscopy (EDS) equipped on SEM. The decoloration rate (DR) of MO and MB is calculated using Equation (1):

$$DR = \frac{C_0 - C_t}{C_0} \times 100 \quad (1)$$

where C_0 is the initial concentration of MO (MB), C_t is the concentration of MO (MB) after t hours of decoloration. The concentration of MO (MB) is proportional to optical absorption intensity (I) at 463 nm (662 nm), i.e.,

$$C = kI \quad (2)$$

where k is a constant. The k of MO and MB is about 19 mg L⁻¹ and 6.4 mg L⁻¹, respectively. The pH of MO and MB aqueous solution is about 7.2 and 6.8, respectively. The mass of ZnO and ZnO-Cu₂O catalyst is about 0.23 g and 0.24 g, respectively.

3. Results and Discussion

Figure 1 shows the SEM of ZnO, Cu₂O, and ZnO-Cu₂O sample in parts a–c, respectively. The ZnO nano-sheets have a thickness of about 90 nm. The nano-sheets are perpendicular to the substrate. There are many micrometer-sized voids in the sample. The voids size in Cu₂O is smaller than that in ZnO. The granule shape in Cu₂O is irregular. The ZnO-Cu₂O shows nano-sheets and irregular particles. The thickness of ZnO-Cu₂O nano-sheets is about 160 nm. The voids size is smaller than that in ZnO. The surface of ZnO is smoother than that of ZnO-Cu₂O. The shape change in nano-sheets should be due to the growth Cu₂O on surface of ZnO nano-sheets. The atomic ratio of Cu to Zn of ZnO-Cu₂O sample determined by EDS is about 9:1.

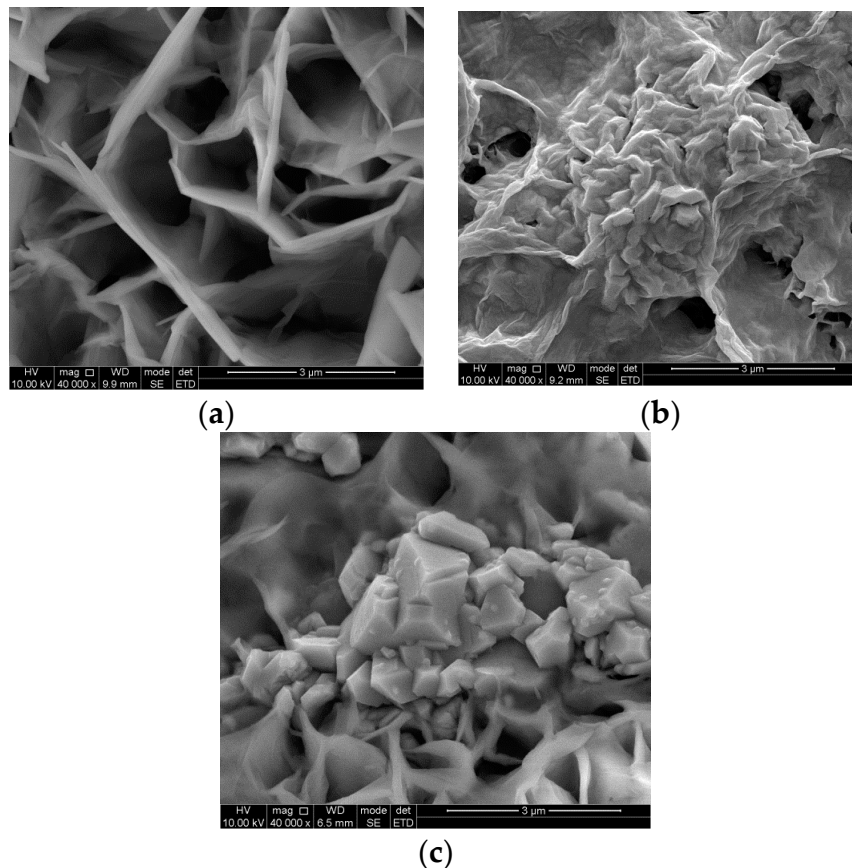


Figure 1. The scanning electron microscopy (SEM) of ZnO (a), Cu₂O (b), and ZnO-Cu₂O (c) sample.

Figure 2 shows the XRD of Al foam, ZnO, Cu₂O and ZnO-Cu₂O sample. The (111), (200), (220), and (311) diffraction peaks of Al foam are from Al metal (JCPDS: 03-0932). The (214), (413), and (244) diffraction peaks of Al foam are from Al₂O₃ oxides (JCPDS: 02-1373). The diffraction peaks of Cu₂O at about 36.7°, 42.4°, 61.7°, and 73.6° are due to (111), (200), (220), and (311) planes of cubic Cu₂O (JCPDS:77-0199), respectively. The crystal size of Cu₂O is determined to be about 160 nm using (111) diffraction with Scherrer formula. The new diffraction peak at about 10.8° in the ZnO sample may be from Al₂O₃ oxides (JCPDS: 02-1373). This indicates that partial aluminum metal is oxidized during the growth of ZnO. The peaks at about 20.5° and 34.8° are from (102) and (104) planes of hexagonal ZnO (JCPDS:01-1136), respectively.

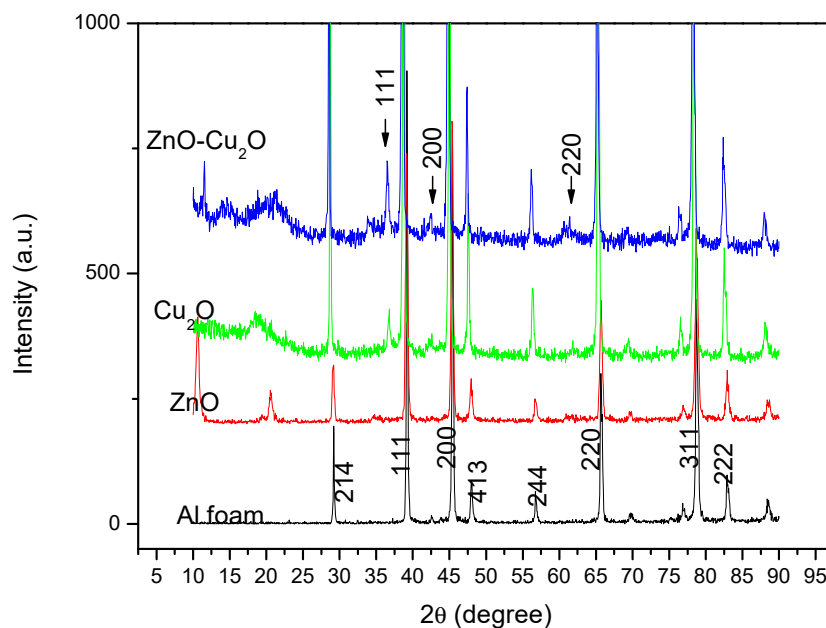


Figure 2. The XRD of aluminum (Al) foam, ZnO, Cu₂O and ZnO-Cu₂O sample.

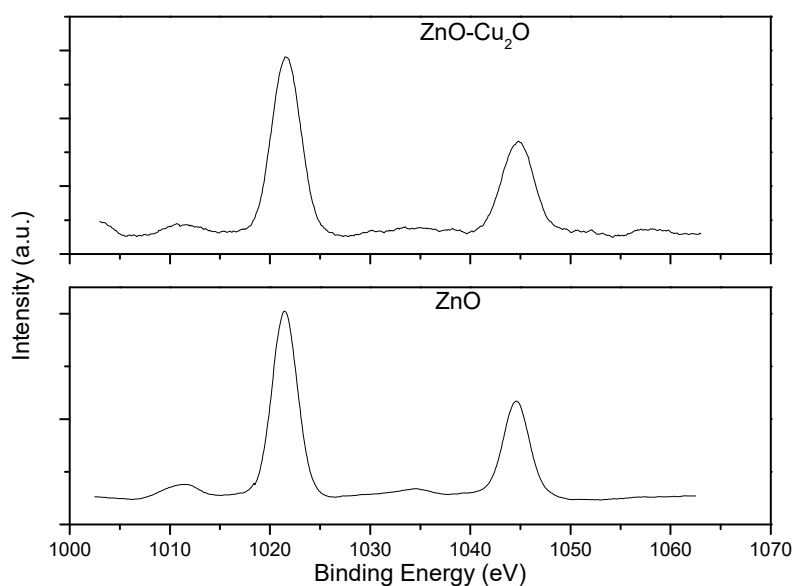


Figure 3. The Zn 2p X-ray photoelectron spectroscopy (XPS) of ZnO and ZnO-Cu₂O.

Figure 3 shows the Zn 2p XPS of ZnO and ZnO-Cu₂O. The binding energy of Zn 2p_{3/2} of ZnO and ZnO-Cu₂O is about 1021.47 and 1021.61 eV, respectively. The binding energy of Zn 2p_{1/2} of ZnO and ZnO-Cu₂O is about 1044.57 and 1044.74 eV, respectively. The binding energy of Zn 2p in ZnO-Cu₂O shifts to higher energy compared with that of ZnO. The shift of binding energy was attributed to the electronic interaction between two materials [18]. Therefore, the shift in binding energy of Zn indicates that there should be intimate contact between the two materials.

Figure 4 shows the optical absorption of MO decolorized by adsorption using ZnO, Cu₂O, and ZnO-Cu₂O as adsorbents in parts a–c, respectively. There are two main optical absorption bands with peaks located at about 463 nm and 272 nm. The band at wavelength of 463 nm was attributed to the conjugated structure constructed via azo bond [19]. The peak's intensity decreases with decolorization time increasing from 0 s to 20 s. A new optical absorption peak appears at about 370 nm for the Cu₂O adsorbents. The new absorption peak is not due to the losing of Cu₂O in solution as there is no absorption peak in the same treated water solution. This indicates that there are other mechanisms

than adsorption presenting in Cu_2O adsorbents [12]. It was demonstrated that MO can be decomposed to xylene and ethylbenzene [12]. Carbon center radicals such as methyl radical and phenyl radical have reconnected with each other to produce xylene or ethylbenzene [12].

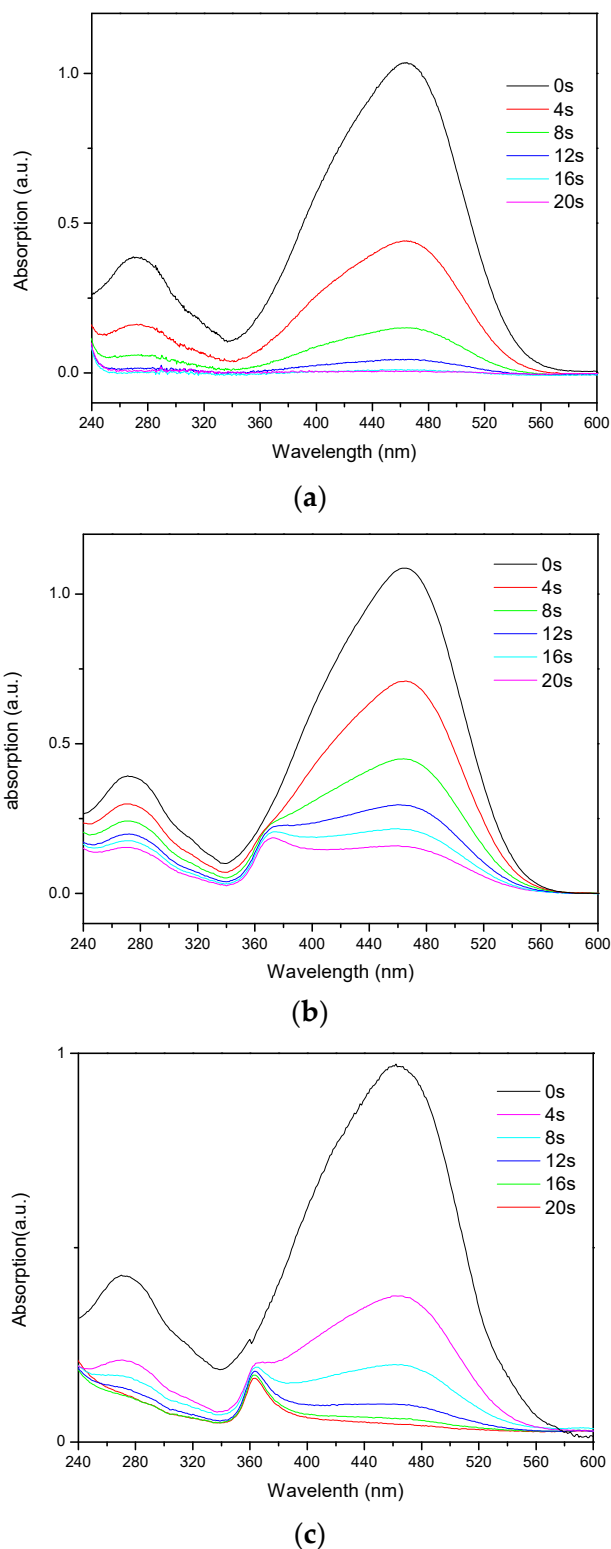


Figure 4. The optical absorption of methyl orange (MO) decolorized by adsorption using ZnO (a), Cu_2O (b), and ZnO- Cu_2O (c) as adsorbents.

Pseudo-first-order kinetics reaction was applied to simulate the experimental data with the Langmuir–Hinshelwood model $\ln(C_0/C) = \alpha t$, where α is the pseudo-first-order rate constant, and was determined from a linear fit to the experimental data [13,20]. Figure 5 shows that experimental data can be fitted well using the pseudo-first-order kinetics. The rate constant α is determined to be about 0.02, 0.129, and 0.275 min^{-1} for Cu_2O , $\text{ZnO-Cu}_2\text{O}$, and ZnO , respectively. The higher α of ZnO indicates that ZnO has the greater adsorption ability towards MO. The weaker adsorption ability of $\text{ZnO-Cu}_2\text{O}$ may be related to the reduction in specific surface area and positive charges on surface [3]. ZnO and Cu_2O are n-type and p-type semiconductors, respectively. The depletion region at the interface of the p-n junction [14] may reduce the positive charges on the surface. The adsorption of MB for Cu_2O , $\text{ZnO-Cu}_2\text{O}$, and ZnO is too small to be detected. The weak adsorption of MB should be due to the positively charged surface of adsorbents [3,21].

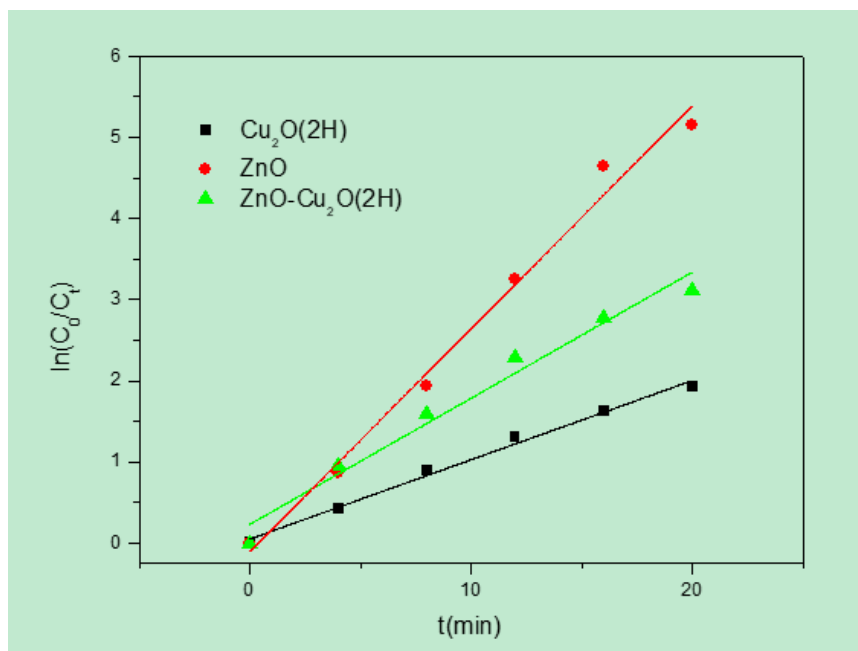


Figure 5. The pseudo-first-order kinetics fit the concentration as a function of time.

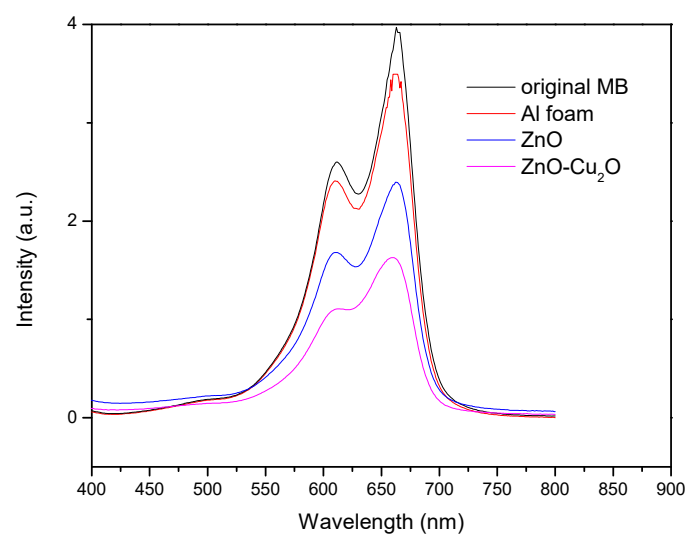


Figure 6. The decolorization of methylene blue (MB) with Al foam, ZnO , and $\text{ZnO-Cu}_2\text{O}$ as catalyst under ultrasonic irradiation.

Figure 6 shows the optical absorption of MB decolorized by Al foam, ZnO, and ZnO-Cu₂O as catalyst under ultrasonic irradiation. The ultrasonic irradiation time is about 24 h. The peak intensity decreases from Al foam, ZnO to ZnO-Cu₂O. DR is about 13%, 40%, and 59% for Al foam, ZnO, and ZnO-Cu₂O catalyst, respectively. DR of MB decolorized by ZnO and ZnO-Cu₂O is larger than that decolorized by Al foam. The enhancement of DR should be due to the piezoelectric potential of ZnO and ZnO-Cu₂O.

Figure 7 shows the decolorization of MB using ultrasonic irradiation. As seen in Figure 7, the DR of ZnO-Cu₂O is much higher than that of ZnO. With 50 h ultrasonic irradiation, DR of ZnO-Cu₂O and ZnO is about 70% and 48%, respectively. This enhancement of DR is related to many factors, such as the cavitation [22] and piezoelectric enhanced vibration catalysis [5]. On the one hand, the weak points in MB solution can be increased by putting a catalyst in it, which in turn leads to increasing nucleation of the cavitation bubbles, the number of free radicals generated, and the rate of degradation of the organic compound [22]. On the other hand, the depletion layer was demonstrated to be of benefit for the enhancement of the output of piezoelectricity [16]. The positive–negative charges are easier to get apart because of the small exciton binding energy with built-in polarization due to piezoelectric effect [5]. Due to the p–n junction of ZnO-Cu₂O, the number of excess electrons in ZnO can be effectively reduced, which is beneficial to the piezoelectric signal output [23]. A 13-fold higher output voltage was achieved in ZnO-Cu₂O nano-generator compared with ZnO [23]. A dramatic increase in H₂ production is caused by decreasing the mobile charge concentration in ZnO piezo-catalysis [24]. Low electrical conductivity is desirable in order to enable high electrochemical activity [24]. The reason of the larger DR of ZnO-Cu₂O may be due to there being a p–n junction and a carrier depletion layer at the interface of ZnO-Cu₂O. The depletion layer can enhance the piezoelectricity and electrochemical activity then increase the DR.

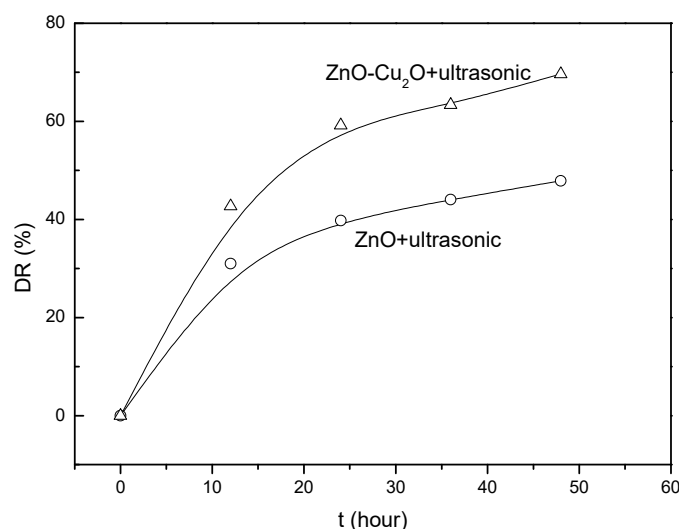


Figure 7. The decolorization of MB using ultrasonic irradiation.

The mechanism of the enhancement of DR by depletion layer is shown in the Figure 8. The density of an electron in pure ZnO is higher than that in a ZnO-Cu₂O junction boundary due to the forming of a depletion region [23]. The piezoelectric potential of pure ZnO is smaller than that of ZnO-Cu₂O because of the piezoelectric potential screening effect due to excessive electrons [16,23,25,26]. The piezoelectric potential [27] and piezoelectrically-induced electric charges [5] could stimulate the decolorization reactions via electrochemical redox reaction. The negative charges (or e⁻) on the surface attract the dissolved oxygen in the water and produce superoxide radicals ($\cdot\text{O}_2^-$). Meanwhile, hydroxyl radicals ($\cdot\text{OH}$) can be released by positive charges (or h⁺) accumulated on the surface [5,27]. The strong oxidative $\cdot\text{O}_2^-$ and $\cdot\text{OH}$ can cause the decolorization reactions of dye [5,27].

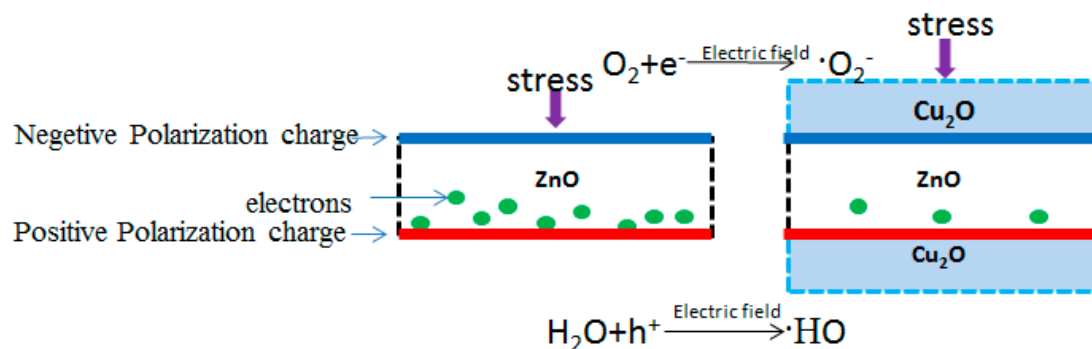


Figure 8. The mechanism of the enhancement of decoloration rate (DR) by depletion layer.

4. Conclusions

It was demonstrated in this paper that the ZnO and ZnO-Cu₂O have good adsorption to anionic dyes, but have weak adsorption to cationic dyes. The hybrid structure of ZnO-Cu₂O improves the sono-catalysis activity of ZnO to decolorize cationic dyes. The p-n junction between ZnO-Cu₂O is shown to be beneficial for the sonocatalysis decolorization of cationic dyes. Since the free electrons in the interface of ZnO-Cu₂O are reduced, it should be the polarized charges, not the free charges, that play the important role in piezo-catalysis.

Author Contributions: C.M.L. conceived and designed the experiments; J.D.D., L.G. and H.Y.Z. performed the experiments; C.M.L. and J.D.D. analyzed the data and wrote the paper.

Funding: This study was supported financially by the Agricultural Public Welfare Project of the Sichuan Province of China (grant no.2015NZ0098) and the Fundamental Research Funds for The Central Universities (grant no.ZYGX2016J062).

Conflicts of Interest: The authors declare no conflict of interest.

References

- Hosseini, A.; Faghihian, H.; Sanati, A.M. Elimination of dibenzothiophene from transportation fuel by combined photocatalytic and adsorptive method. *Mater. Sci. Semicond. Process.* **2018**, *87*, 110–118. [[CrossRef](#)]
- Singh, G.; Singh, J.; Jolly, S.S.; Rawat, R.; Kukkar, D.; Kumar, S.; Basu, S.; Rawat, M. Fructose modified synthesis of ZnO nanoparticles and its application for removal of industrial pollutants from water. *J. Mater. Sci. Mater. Electron.* **2018**, *29*, 7364–7371. [[CrossRef](#)]
- Chouchene, B.; Chaabane, T.B.; Mozet, K.; Girot, E.; Corbel, S.; Balan, L.; Medjahdi, G.; Schneider, R. Porous Al-doped ZnO rods with selective adsorption properties. *Appl. Surf. Sci.* **2017**, *409*, 102–110. [[CrossRef](#)]
- Hassanzadeh-Tabrizi, S.A.; Motlagh, M.M.; Salahshour, S. Synthesis of ZnO/CuO nanocomposite immobilized on -Al₂O₃ and application for removal of methyl orange. *Appl. Surf. Sci.* **2016**, *384*, 237–243. [[CrossRef](#)]
- Xu, X.; Jia, Y.; Xiao, L.; Wu, Z. Strong vibration-catalysis of ZnO nanorods for dye waste water decolorization via piezo-electro-chemical coupling. *Chemosphere* **2018**, *193*, 1143–1148. [[CrossRef](#)]
- Qian, W.; Wu, Z.; Jia, Y.; Hong, Y.; Xu, X.; You, H.; Zheng, Y.; Xia, Y. Thermo-electrochemical coupling for room temperature thermocatalysis in pyroelectric ZnO nanorods. *Electrochem. Commun.* **2017**, *81*, 124–127. [[CrossRef](#)]
- Hong, D.; Zang, W.; Guo, X.; Fu, Y.; He, H.; Sun, J.; Xing, L.; Liu, B.; Xue, X. High Piezo-photocatalytic Efficiency of CuS/ZnO Nanowires Using Both Solar and Mechanical Energy for Degrading Organic Dye. *ACS Appl. Mater. Interfaces* **2016**, *8*, 21302–21314. [[CrossRef](#)]
- Song, X.M.; Yuan, C.; Wang, Y.; Wang, B.; Mao, H.; Wu, S.; Zhang, Y. ZnO/CuO photoelectrode with n-p heterogeneous structure for photoelectrocatalytic oxidation of formaldehyde. *Appl. Surf. Sci.* **2018**, *455*, 181–186. [[CrossRef](#)]
- Muzakki, A.; Shabrany, H.; Saleh, R. Synthesis of ZnO/CuO and TiO₂/CuO nanocomposites for light and ultrasound assisted degradation of a textile dye in aqueous solution. *AIP Conf. Proc.* **2015**, *1725*, 020051.
- Gupta, V.K.; Suhas. Application of low-cost adsorbents for dye removal—A review. *J. Environ. Manag.* **2009**, *90*, 2313–2342. [[CrossRef](#)]

11. Ikeda, S.; Takata, T.; Komoda, M.; Hara, M.; Kondo, J.N.; Domen, K.; Tanaka, A.; Hosono, H.; Kawazoe, H. Mechano-catalysis a novel method for overall water splitting. *Phys. Chem. Chem. Phys.* **1999**, *1*, 4485–4491. [[CrossRef](#)]
12. Guo, B.; Liu, G.; Zeng, Y.; Dong, G.; Wang, C. Rapid mineralization of methyl orange by nanocrystalline-assembled mesoporous Cu₂O microspheres. *Nanotechnology* **2018**, *29*, 445701. [[CrossRef](#)]
13. Wang, Y.; Gao, J.; Wang, X.; Jin, L.; Fang, L.; Zhang, M.; He, G.; Sun, Z. Facile synthesis of core-shell ZnO/Cu₂O heterojunction with enhanced visible light-driven photocatalytic performance. *J. Sol-Gel Sci. Technol.* **2018**, *88*, 172–180. [[CrossRef](#)]
14. Ghamgosar, P.; Rigoni, F.; You, S.; Dobryden, I.; Kohan, M.G.; Pellegrino, A.L.; Concina, I.; Almqvist, N.; Malandrino, G.; Vomiero, A. ZnO-Cu₂O core-shell nanowires as stable and fast response photodetectors. *Nano Energy* **2018**, *51*, 308–316. [[CrossRef](#)]
15. Shi, S.; Xu, J.; Li, L. Preparation and photocatalytic activity of ZnO nanorods and ZnO/Cu₂O nanocomposites. *Main Group Chem.* **2017**, *16*, 47–55. [[CrossRef](#)]
16. Wang, Q.; Qiu, Y.; Yang, D.; Li, B.; Zhang, X.; Tang, Y.; Hu, L. Improvement in piezoelectric performance of a ZnO nanogenerator by modulating interface engineering of CuO-ZnO heterojunction. *Appl. Phys. Lett.* **2018**, *113*, 053901. [[CrossRef](#)]
17. Pang, Y.L.; Abdullah, A.Z.; Bhatia, S. Review on sonochemical methods in the presence of catalysts and chemical additives for treatment of organic pollutants in wastewater. *Desalination* **2011**, *277*, 1–14. [[CrossRef](#)]
18. Ye, F.; Li, H.; Yu, H.; Chen, S.; Quan, X. Hydrothermal fabrication of few-layer MoS₂ nanosheets within nanopores on TiO₂ derived from MIL-125(Ti) for efficient photocatalytic H₂ evolution. *Appl. Surf. Sci.* **2017**, *426*, 177–184. [[CrossRef](#)]
19. Chen, Y.P.; Liu, S.Y.; Yu, H.Q.; Yin, H.; Li, Q.R. Radiation-induced degradation of methyl orange in aqueous solutions. *Chemosphere* **2008**, *72*, 532–536. [[CrossRef](#)]
20. Jing, H.Y.; Wen, T.; Fan, C.M.; Gao, G.Q.; Zhong, S.L.; Xu, A.W. Efficient adsorption/photodegradation of organic pollutants from aqueous systems using Cu₂O nanocrystals as a novel integrated photocatalytic adsorbent. *J. Mater. Chem. A* **2014**, *2*, 14563. [[CrossRef](#)]
21. Chen, D.S.; Yu, W.B.; Deng, Z.; Liu, J.; Jin, J.; Li, Y.; Wu, M.; Chen, L.H.; Su, B.L. Hollow Cu₂O microspheres with two active {111} and {110} facets for highly selective adsorption and photo degradation of anionic dye. *RSC Adv.* **2015**, *5*, 55520. [[CrossRef](#)]
22. Liu, C.M.; Huang, X.Y.; Zhang, H.Y.; Dai, J.D.; Ning, C.C. The decoloration of methyl orange using aluminum foam, ultrasound and direct electric current. *Mater. Res. Express* **2018**, *5*, 015501. [[CrossRef](#)]
23. Lei, J.; Yin, B.; Qiu, Y.; Zhang, H.; Chang, Y.; Luo, Y.; Zhao, Y.; Ji, J.; Hu, L. Flexible piezoelectric nanogenerator based on Cu₂O-ZnO p-n junction for energy harvesting. *RSC Adv.* **2015**, *5*, 59458. [[CrossRef](#)]
24. Starr, M.B.; Wang, X. Fundamental Analysis of Piezocatalysis Process on the Surfaces of Strained Piezoelectric Materials. *Sci. Rep.* **2013**, *3*, 2160. [[CrossRef](#)] [[PubMed](#)]
25. Lee, K.; Kumar, Y.B.; Seo, J.S.; Kim, K.H.; Sohn, J.I.; Cha, S.N.; Choi, D.; Wang, Z.L.; Kim, S.W. p-type polymer-hybridized highperformance piezoelectric nanogenerators. *Nano Lett.* **2012**, *12*, 1959. [[CrossRef](#)] [[PubMed](#)]
26. Shin, S.H.; Lee, M.; Jung, J.Y.; Seol, J.; Nah, J. Piezoelectric performance enhancement of ZnO flexible nanogenerator by a CuO-ZnO p-n junction formation. *J. Mater. Chem. C* **2013**, *1*, 8103–8107. [[CrossRef](#)]
27. Wu, J.M.; Chang, W.E.; Chang, Y.T.; Chang, C.K. Piezo-Catalytic Effect on the Enhancement of the Ultra-High Degradation Activity in the Dark by Single and Few-Layers MoS₂ Nanoflowers. *Adv. Mater.* **2016**, *28*, 3718–3725. [[CrossRef](#)] [[PubMed](#)]

